



Membrane flux dynamics in the submerged ultrafiltration hybrid treatment process during particle and natural organic matter removal

Wei Zhang^{1,2}, Xiaojian Zhang¹, Yonghong Li¹, Jun Wang¹, Chao Chen^{1,*}

1. Department of Environmental Science and Engineering, Tsinghua University, Beijing 100084, China. E-mail: chen_water@tsinghua.edu.cn

2. Beijing Special Engineering Design and Research Institute, Beijing 100028, China

Received 19 December 2010; revised 28 February 2011; accepted 01 March 2011

Abstract

Particles and natural organic matter (NOM) are two major concerns in surface water, which greatly influence the membrane filtration process. The objective of this article is to investigate the effect of particles, NOM and their interaction on the submerged ultrafiltration (UF) membrane flux under conditions of solo UF and coagulation and PAC adsorption as the pretreatment of UF. Particles, NOM and their mixture were spiked in tap water to simulate raw water. Exponential relationship, ($J_p/J_{p0} = a \times \exp\{-k[t-(n-1)T]\}$), was developed to quantify the normalized membrane flux dynamics during the filtration period and fitted the results well. In this equation, coefficient a was determined by the value of J_p/J_{p0} at the beginning of a filtration cycle, reflecting the flux recovery after backwashing, that is, the irreversible fouling. The coefficient k reflected the trend of flux dynamics. Integrated total permeability (ΣJ_p) in one filtration period could be used as a quantified indicator for comparison of different hybrid membrane processes or under different scenarios. According to the results, there was an additive effect on membrane flux by NOM and particles during solo UF process. This additive fouling could be alleviated by coagulation pretreatment since particles helped the formation of flocs with coagulant, which further delayed the decrease of membrane flux and benefited flux recovery by backwashing. The addition of PAC also increased membrane flux by adsorbing NOM and improved flux recovery through backwashing.

Key words: ultrafiltration; membrane flux; particles; natural organic matter; hybrid process; backwashing

DOI: 10.1016/S1001-0742(10)60622-5

Citation: Zhang W, Zhang X J, Li Y H, Wang J, Chen C, 2011. Membrane flux dynamics in the submerged ultrafiltration hybrid treatment process during particle and natural organic matter removal. *Journal of Environmental Sciences*, 23(12): 1970–1976

Introduction

Turbidity-causing particles and natural organic matter (NOM) are two major concerns in surface water, and can influence membrane flux and lead to membrane fouling during ultrafiltration (UF) processes. The mechanism of particle fouling is described as filtration cake layer formation. Particles in natural water sources are inorganic in origin and are bigger than the UF membrane pore. Therefore, particles cannot pass through the membrane pores, which means that particle fouling is reversible and can be revived effectively by backwashing.

Natural organic matter has a large negative impact on the efficiency of UF membranes (Nghiem et al., 2006), is usually not removed by the UF process, and contributes to membrane fouling (Campinas and Rosa, 2010). Fouling mechanisms of NOM include gel formation (an extreme case of concentration-polarization), cake formation, pore blockage, and constriction (Cho et al., 1999). Factors potentially affecting membrane fouling by NOM include the properties of feed constituents (molecular weight dis-

tribution, hydrophilicity and charge density) and that of membranes (hydrophilicity, surface roughness, porosity) (Kim et al., 2006). Considering membrane pore size, the size distribution of feed solution components is especially important. Foulants smaller than the membrane pores may be adsorbed on pore wall and lead to pore constriction, while larger components may block pore entrances and contribute to cake or gel formation on the membrane surface (Nghiem et al., 2006; Costa et al., 2006).

To reduce membrane fouling and increase flux, it is necessary to develop hybrid treatment processes which combine UF with conventional water treatment techniques, such as coagulation and powdered activated carbon (PAC) adsorption (Costa and De Pinho, 2004; Tomaszewska and Mozia, 2002; Dong et al., 2007; Zhang et al., 2003). Coagulation can relieve membrane fouling through pollutant removal and flocs formation. The combination of UF with PAC is a promising water treatment option as UF is a safe barrier against bacteria, viruses, and cyanobacteria while PAC is efficient for soluble organic removal, thus reducing NOM adsorption on the membrane surface and/or pores (Nghiem et al., 2006).

* Corresponding author. E-mail: chen_water@tsinghua.edu.cn

Most fouling studies have focused either on NOM fouling or particle fouling alone. Some papers on membrane filtration treating mixtures of NOM-particle solution have recently been published. For example, particle aggregation/stabilization by NOM and hindered NOM back-diffusion were found to play an important role during NF filtration (Duclos-Orsello et al., 2006). Jermann et al. (2008) studied the interaction between particles and NOM in the inside-out UF filtration. Many researchers have studied the effect of coagulation and PAC adsorption as a pretreatment of UF for membrane fouling (Matsui et al., 2004; Howe et al., 2006), with some finding that PAC increased membrane flux (Xia et al., 2007), while some found that PAC aggravated membrane performance (Zhao et al., 2005). However, most research has focused on the inside-out and pressured UF membranes, with few reports on submerged membrane fouling by the interaction between particles and NOM (Duclos-Orsello et al., 2006).

The objective of this article was to investigate the effect of particles, NOM and their interaction on submerged UF membrane flux under conditions of solo UF and coagulation and PAC adsorption as a UF pretreatment.

1 Materials and methods

1.1 Membrane filtration and affiliated equipment

Figure 1 illustrates the schematic diagram of the UF experimental equipment. The system consisted of UF membrane modules, raw water preparation system, coagulant or PAC feeding system, and air-water backwashing system.

In this study, one submerged hollow fiber UF membrane module with a total membrane area of 4 m² was employed. The membrane fiber was made of polyvinylidene fluoride (PVDF) and was 400 mm long with a pore size of 0.03 μm, inside diameter of 0.6 mm and outside diameter of 1.0 mm.

The concentration of foulants in raw water, particles, and NOM, was controlled by adjusting the flow rate of tap water and that of stock solution. Raw water flowed into the coagulation tank by gravity. Coagulant

(Al₂(SO₄)₃·18H₂O) or PAC smaller than 200 mesh was dosed into the pipe between the raw water tank and the coagulation tank. After coagulation, the water flowed into the membrane filtration tank. The treated water was driven through the membrane by one diaphragm pump, an air conduit with holes downwards was installed under the membrane module in the tank, through which air was pumped to clean the membrane fiber intermittently. Backwashing was carried out regularly by a backwashing pump. The equipment worked automatically with a programmable logic controller (PLC). The flow rate was measured by a flow meter. A pressure sensor was set between the membrane module and the diaphragm pump to monitor the trans-membrane pressure (TMP).

In this experiment, membrane flux was set as 45 L/(m²·hr). The interval and the duration of the aeration were 2 min and 15 sec, respectively. The aeration intensity was about 8 m³/(m²·hr). One filtration cycle lasted 2 hr and was followed by 2 min backwashing with aeration. The backwashing intensity was 80 L/(m²·hr).

1.2 Particles and NOM

In this experiment, particles in raw water were simulated by kaolinite. Kaolinite solution of 5 g/L was prepared in the stock solution tank and diluted in the raw water tank with tap water. The diameters of the particles were determined by an EyeTech laser particle analyzer (Ankersmid, Holland) (Fig. 2). The diameters of almost all particles in the simulated raw water were above 0.3 μm.

Humic acid (HA) (Tianjing Jinke Fine Chemical Institute, China) extracted from the lixivium of straw was used as the NOM model compound. We dissolved 17 g HA in 10 L tap water as stock solution by aiding of pH = 10 and 80°C. Later, the stock solution was fed with tap water in different dilution rates. In this study, the concentration of NOM was presented by UV₂₅₄ absorbance. The apparent molecular weight (AMW) of the humic acid was determined by Millipore 8200 stirred ultrafiltration cells and UF membranes by cutting off molecular weight of 100, 30, 10, 5, 3, 1 kDa, respectively (Millipore, USA). The percentage of each fraction of HA in the stock solution mentioned above is presented in Fig. 3.

1.3 Analysis methods

The UV absorbance at 254 nm (UV₂₅₄) was measured by an UV/Vis spectrophotometer (T6, Persee, China) after

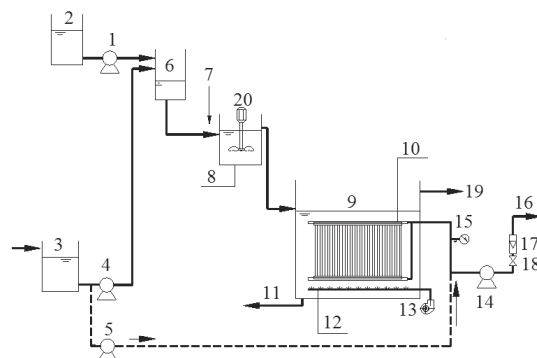


Fig. 1 Schematic flow diagram of the experiment. (1) peristaltic pump; (2) humic acid or kaolinite stock solution; (3) tap water tank; (4) centrifugal pump; (5) backwashing pump; (6) raw water tank; (7) feed pipe of coagulation or PAC; (8) coagulation tank; (9) membrane filtration tank; (10) membrane module; (11) discharge; (12) aerated conduit; (13) air pump; (14) diaphragm pump; (15) pressure sensor; (16) treated water; (17) flow meter; (18) valve; (19) overflow pipe; (20) stirrer.

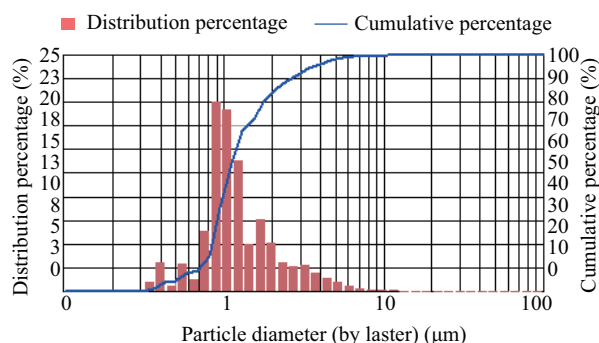
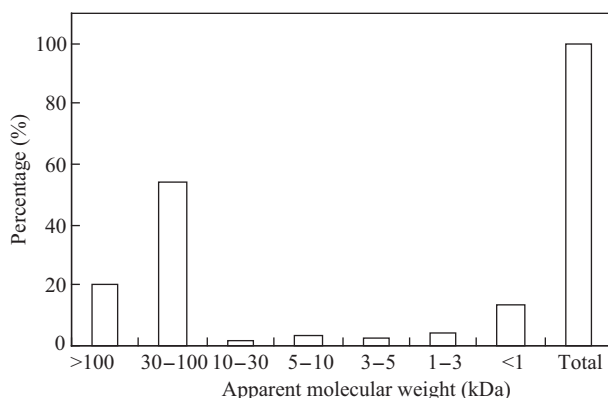


Fig. 2 Distribution of particle diameters in the simulated raw water.

Table 1 Comparison of different membrane filtration processes

Raw water	Basic water quality		Processes					
			Solo UF		Coagulation/UF		PAC/UF	
	Turbidity (NTU)	UV ₂₅₄ (cm ⁻¹)	Al ³⁺ (mg/L)	PAC (mg/L)	Al ³⁺ (mg/L)	PAC (mg/L)	Al ³⁺ (mg/L)	PAC (mg/L)
Particle	20		0	0	2	0	0	20
NOM		0.25	0	0	2	0	0	20
Particle + NOM	20	0.25	0	0	2	0	0	20

NOM: natural organic matter; UF: ultrafiltration; PAC: powdered activated carbon.

**Fig. 3** Molecular weight distribution of the NOM.

the sample was filtered with 0.45 μm membrane. Turbidity was measured by a portable turbidity meter (2100P HACH, USA). Morphological analysis of the fouled membranes before and after physical backwashing was performed by scanning electronic microscope (SEM, JSM-6460LV, Japan).

1.4 Experimental design

Three kinds of raw water were prepared: kaolinite solution, HA solution, and a mixture of kaolinite and HA. Three processes were compared with each other: solo UF, coagulation/UF and PAC/UF. The process comparison scheme is presented in Table 1.

2 Results

2.1 Pollutant removal

The turbidities of the effluents in each process were all below 0.1 NTU, due to retention characteristics of the particles by the UF membrane. The removal rates of UV₂₅₄ in each process are shown in Table 2.

2.2 Flux dynamic curves in the filtration period

Flux dynamics determined the capacity of the membrane filtration process, which was the primary goal of UF process. Thus, permeate flux was monitored over time to determine the effect of membrane fouling on membrane permeability. Parameters used to quantify the efficiency of membrane processes were permeate flux (J), permeability (J_P , L/(m²·hr·kPa)) and the normalized permeate flux (J_P/J_{P0}). Flux of membrane filtration is defined as Eq. (1):

$$J = \frac{Q}{A} \quad (1)$$

Table 2 Removal rates of UV₂₅₄ in each process

Raw water	Removal rate (%)		
	Solo UF	Coagulation/UF	PAC/UF
NOM	15.0	60.7	19.5
Kaolinite + NOM	16.2	87.2	20.2

where, Q (L/hr) is the permeate flow rate and A (m²) is the membrane area.

Permeability of membrane filtration is defined as Eq. (2):

$$J_P = \frac{Q}{A \times P} \quad (2)$$

where, P (kPa) is the TMP.

The flux dynamics of the UF membrane filtration were studied in terms of the normalized permeate flux J_P/J_{P0} , which was dimensionless and J_{P0} is the initial of the fresh membrane. The degree of the membrane fouling can be presented through the change of J_P/J_{P0} . Normalized permeate flux dynamic curves of each process were used as the benchmark for comparison, as illustrated in Fig. 4.

2.3 Data fitting

According to Fig. 4, the curves of flux dynamics in each cycle fitted the exponential equation well. This equation fitted the complete pore blockage model described by Duclos et al. (2006), in which the flux was shut off by the deposition of foulant aggregates on the membrane surface and the filtrate could only pass through the unblocked pore area. The fitting equation is described as Eq. (3):

$$J_P/J_{P0} = a \times \exp\{-k[t - (n - 1)T]\} \quad (3)$$

where, the coefficient a is the value of J_P/J_{P0} at the beginning of one cycle in the process, which reflects the revival of J_P/J_{P0} after backwashing. The value of a at the first cycle of each process was 1 and the value of a at the sequential cycles varied due to the different pretreatment adopted or different pollutants treated. The coefficient k represents the decline velocity of J_P/J_{P0} , with a larger k value meaning permeability (J_P) decreased faster. The coefficient k reflected the curve of flux dynamic and was used as a quantified indicator for comparison of membrane fouling under different situations. The t is time, T is the length of one cycle including filtration and backwashing, and n is the cycle number. To investigate flux decline and the effect of backwashing simultaneously, the data of flux dynamic in the second cycle was fitted. Table 3 shows the

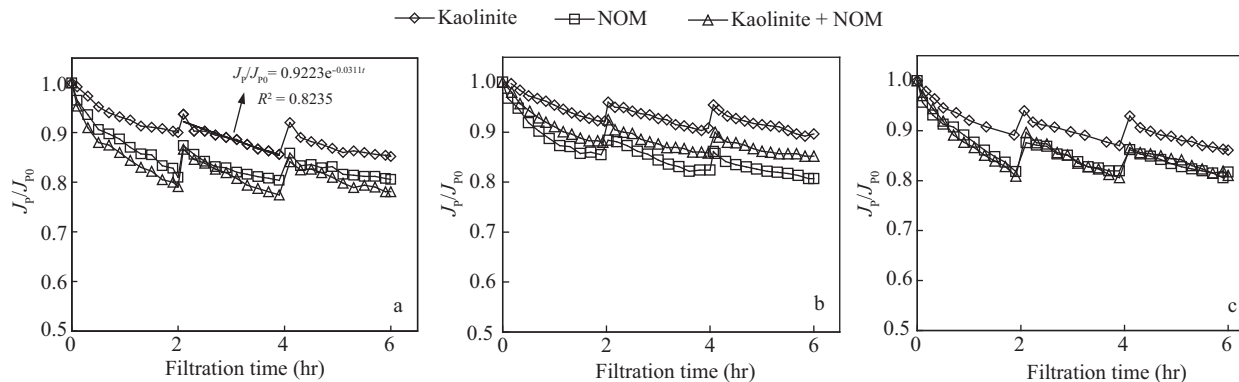


Fig. 4 Normalized permeate flux in solo UF (a), coagulation/UF (b), and PAC/UF (c) processes with foulants as indicated.

Table 3 Values of a , k from fitting equation in each course

Raw water	UF			Coagulation/UF			PAC/UF		
	a	k	R^2	a	k	R^2	a	k	R^2
Kaolinite	0.9223	0.0311	0.8235	0.9572	0.0305	0.9757	0.9286	0.0327	0.9459
NOM	0.8651	0.0429	0.9254	0.8842	0.0411	0.9559	0.8810	0.0421	0.9656
Kaolinite + NOM	0.8646	0.0610	0.9867	0.9120	0.0344	0.9867	0.8952	0.0575	0.9827

value of a , k and related coefficient (R^2) from the fitting equations in each course shown in Fig. 4.

To investigate the total permeability (ΣJ_P) during one filtration cycle of each process, Eq. (3) was integrated as follows:

$$\begin{aligned}
 \sum J_P &= \int_{t_1}^{t_2} J_P dt \\
 &= J_{P0} \times \int_{t_1}^{t_2} a \times \exp\{-k[t - (n-1)T]\} dt \\
 &= \frac{J_{P0} \times a}{k} \exp\{-k[t - (n-1)T]\} \Big|_{t_1}^{t_2} \\
 &= \frac{J_{P0} \times a}{k} \{\exp\{-k[t_2 - (n-1)T]\} - \exp\{-k[t_1 - (n-1)T]\}\}
 \end{aligned} \quad (4)$$

For one integrated filtration cycle of each process, $t_2 = nT$, and $t_1 = (n-1)T$, and then $\exp\{-k[t_2 - (n-1)T]\} - \exp\{-k[t_1 - (n-1)T]\} = \exp(-2k) - 1$, let $B = \frac{a}{k}[\exp(-2k) - 1]$, then,

$$\sum J_P = B \times J_{P0} \quad (5)$$

Equation (5) indicates that B determines the total permeability of each process or under each scenario. For example, if pure water passed through the membrane and there was no membrane flux decline, then $J_P/J_{P0} = 1$, $t_2 - t_1$ (each filtration cycle) = 2 hr, and $\sum J_P = \int_{t_1}^{t_2} J_P dt = J_{P0} \times \int_{t_1}^{t_2} dt = J_{P0} \times \int_0^2 dt = 2J_{P0}$, i.e., $B_{\text{pure}} = 2$, then B/B_{pure} was the percentage of total permeability between treating raw water and pure water. By this means, total permeability of each process in a certain filtration cycle could be compared directly, as summarized in Fig. 5.

According to Fig. 5, the addition of coagulant or PAC alleviated the declining trend effectively. Solo UF suffered an obvious decline in total flux by kaolinite, NOM, and their mixture. The integrated flux value B/B_{pure} of the

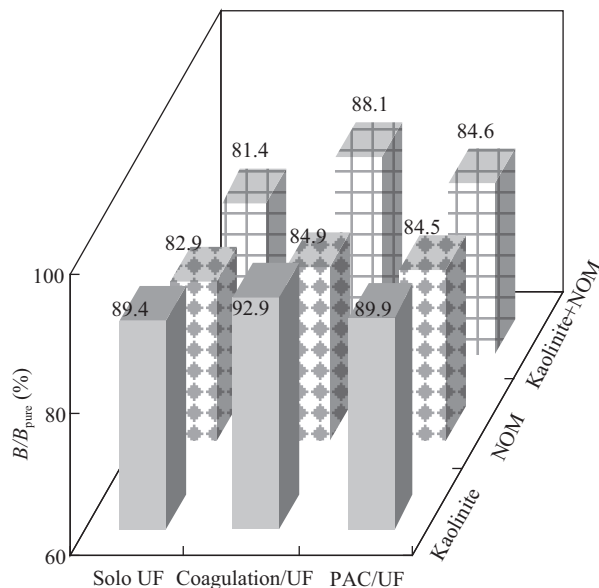


Fig. 5 Comparison of total permeability by B/B_{pure} of different hybrid UF processes.

second turn decreased from 100% to 89.4%, 82.9%, and 81.4%, respectively. Coagulant showed good removal of kaolinite and the mixture of kaolinite and NOM. Flux was improved by 6.7% (from 81.4% to 88.1%) compared with solo UF under this scenario. In addition, PAC also performed well in removing NOM but not as well as coagulant when addressing the mixture.

2.4 SEM images

A SEM image provides information about mechanisms on a microcosmic scale. The SEM images of fresh membrane, membrane fouled by kaolinite, NOM, and pre-mixture of NOM and kaolinite are illustrated in Fig. 6. The surface of the fresh membrane was very smooth. The surface of the membrane fouled by kaolinite alone was covered by cumulate and impacted particles. The cake layer on the membrane surface fouled by NOM alone was

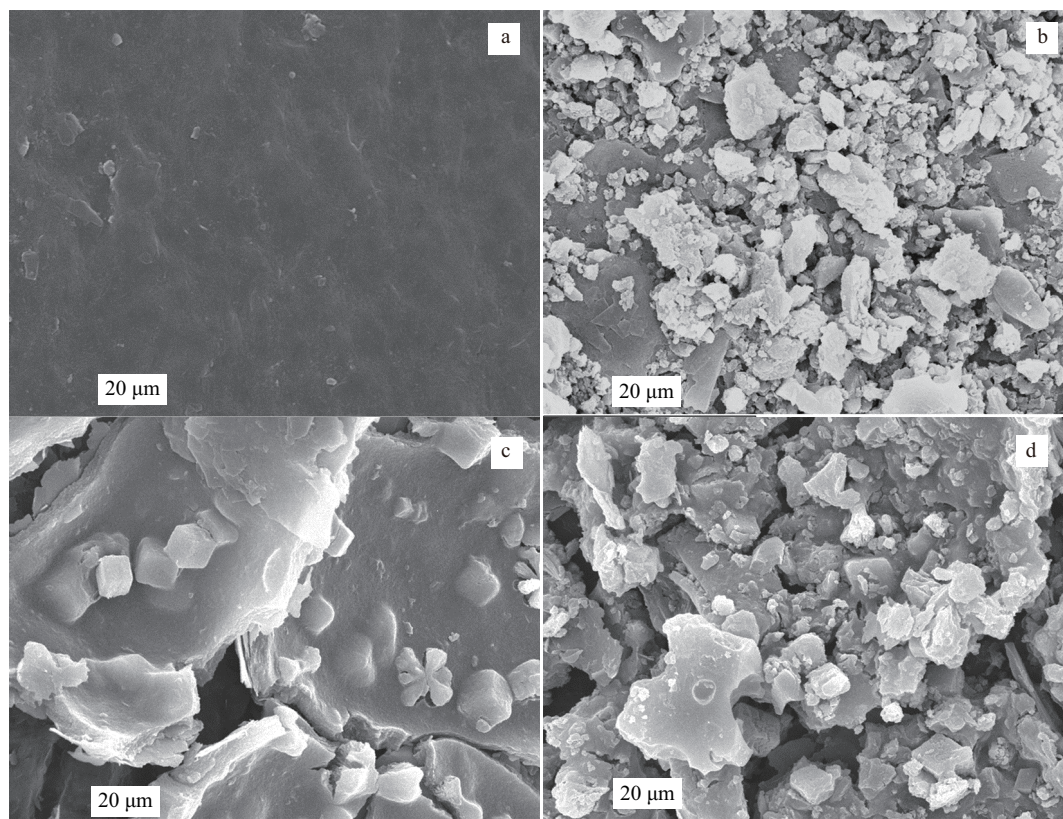


Fig. 6 SEM images of new members (a) and membranes fouled by kaolinite (b), NOM (c) and pre-mixture of NOM and kaolinite (d). The crack of layer was caused by the drying procedure of SEM preparation.

built up by the compact gel-like layer. Figure 6d reveals some uneven matter covering the surface of the membrane.

3 Discussion

3.1 Kaolinite and humic acid

According to Fig. 4a and Table 3, it can be seen that kaolinite alone caused only a minor flux decrease, whereas both HA and kaolinite + HA led to substantial fouling in solo UF. The sequence of coefficients, $k_{\text{kaolinite}}$ (0.0311) $< k_{\text{HA}}$ (0.0429) $< k_{\text{kaolinite} + \text{HA}}$ (0.061), $B_{\text{kaolinite}}$ (1.79) $> B_{\text{HA}}$ (1.66) $> B_{\text{kaolinite} + \text{HA}}$ (1.63), indicated an additive fouling effect between HA and kaolinite. While removing mixture of kaolinite and HA, the coefficient a was higher than that when removing HA alone. In Fig. 4b and Table 3, kaolinite alone also caused a minor flux decline and both scenarios with HA led to substantial flux decline in the coagulation/UF process. However, flux decline by the mixture of HA and kaolinite for this process was slightly lower than that by HA alone ($k_{\text{kaolinite} + \text{HA}}$ (0.0344) $< k_{\text{HA}}$ (0.0411)).

According to Fig. 1, the diameter of kaolinite ($> 0.3 \mu\text{m}$) was bigger than that of the membrane pore ($0.03 \mu\text{m}$). Particles could not enter the pore and thus formed a cake layer on the membrane surface (Fig. 6b). The decline of J_p/J_{p0} was related with the thickness, density and porosity of the cake layer, which developed continually with the increase of filtrate volume, which related to the fact that the surface of kaolinite was heterogeneous and had negatively charged basal faces but conditional charged edges. At neutral pH values, edge-to-face aggregates can be formed, leading to a

polyhedral face-edge structure (Jermann et al., 2008). This kind of structure resulted in relatively large porosity of the cake layer with a relatively high hydraulic permeability (Tombácz et al., 2004). The particles of kaolinite could only form loose physical deposits rather than firm chemical bonds or sticky materials upon membrane surfaces, which made the foulants on the surface of the membrane easy to be removed by backwashing. This explains why the coefficient a was larger when removing kaolinite, as shown in Table 2.

The mechanisms of NOM fouling include gel formation, cake formation, pore blockage, and pore constriction (Cho et al., 1999). In general, NOM components smaller than the membrane pores can be adsorbed onto the inner surfaces and benefit the flux decline while larger components block the pore entrances and contribute to cake formation (Campinas et al., 2010). As NOM molecules accumulated on the surface of the membrane and formed the cake layer (Fig. 6c), flux declined continually with filtration volume. Due to the strong binding force between membrane and foulants, flux decline by NOM was relatively difficult to recover.

With the co-existence of particles and NOM, NOM will adsorb onto the surface of the particles, increase particle stability, decrease the agglomerate size, and smooth out surface heterogeneity of kaolinite (Tombácz et al., 2004). Thus a compact cake layer rather than a porous polyhedral structure was formed on the membrane surface (Fig. 6d), which rapidly decreased flux. Coagulation destabilized the particles in the mixture, which made the porous structure reform. Moreover, the flocs adsorbed part of the NOM

molecule and retarded the formation of the cake layer. It is interesting to note that the coefficient of k with the mixture of NOM and kaolinite was less than that with NOM alone. This indicated that particles in the mixture aided floc formation and helped coagulation to better alleviate membrane fouling by NOM.

3.2 Effect of coagulation as pretreatment

Coagulation as a pretreatment of UF improved UV_{254} removal rates obviously, as shown in Table 2, especially for the mixture of kaolinite and NOM. It can also be observed from Table 3 and Fig. 5 that the addition of coagulant as a pretreatment effectively alleviated the declining trend. The coefficient k values of coagulation/UF removing particles, NOM, and their mixture were less than those of solo UF, indicating this pretreatment retarded flux decline during filtration. The coefficient a values of coagulation/UF process were larger than those of solo UF, indicating that coagulation improved flux revival after backwashing. In addition, its total permeability (ΣJ_P), described as B/B_{pure} , during filtration was larger than solo UF when removing particles, NOM, and their mixture.

During coagulation, Al^{3+} neutralized the negative charge on the surface of the colloidal particles and NOM material in the water, which caused the colloids to destabilize and aggregate into flocs. Flocs loosened the cake layer on the membrane surface, which decreased resistance and reduced membrane fouling. At the same time, the binding force between flocs and membrane was weaker than that between pollutants and membrane, thus, the pollutants on the membrane surface were easier to remove and membrane flux was recovered easily by backwashing (Dong et al., 2007).

3.3 Effect of PAC adsorption as pretreatment

Using PAC also improved UV_{254} removal rates, as shown in Table 2, although its effect was not better than coagulation. From Table 3 and Fig. 5, it can be observed that the addition of PAC pretreatment also effectively alleviated the declining trend under NOM existence. All a and B/B_{pure} values for PAC/UF were larger than those of solo UF and the coefficient k values were smaller than those of solo UF, except for removing particles only. This result showed that PAC improved flux revival after backwashing and increased total permeability (ΣJ_P) during one filtration period.

Membrane pores were blocked or narrowed by NOM molecules, which made it difficult to remove small molecule by backwashing. Fortunately, PAC adsorbs small (especially molecular weight > 500 Da) and non-polar NOM molecules, thus preventing them from entering the membrane pore and forming irreversible fouling (Hu et al., 2010). The deposited PAC particles on the membrane surface acted as the skeleton of the cake layer, which loosened the gel material and improved its removal by backwashing.

However, PAC also contributed to the decrease in flux when removing particles alone. As a kind of particle, PAC was deposited on the membrane surface and formed a cake

layer with kaolinite particles. Fortunately, the diameters of the PAC particles (Table 2) were too big to block the membrane pores (Tomaszewska and Mozia, 2002) and the viscosity of the PAC particles was small. Binding force between PAC-formed cake layer and UF membrane was faint. Thus, the cake layer was stripped easily by backwashing and better flux recovery was obtained.

4 Conclusions

(1) The turbidity of UF effluent was always below 0.1 NTU. The UF alone had fairly limited efficiency for NOM removal, while PAC or coagulation pretreatment improved the removal rate greatly.

(2) The exponential relationship ($J_P/J_{P0} = a \times \exp\{-k[(n-1)T]\}$) was applied to quantify the flux dynamics of different hybrid UF processes. Coefficient a was determined by the value of J_P/J_{P0} at the beginning of a filtration cycle, reflecting flux recovery after backwashing, in other words, the irreversible fouling. Coefficient k reflected the trend of flux dynamics. Integrated total permeability (ΣJ_P) in one filtration period was used as a quantified indicator for comparison of different hybrid membrane processes or different scenarios.

(3) Both coagulation and PAC pretreatment had a positive effect on alleviating membrane fouling and maintaining high flux. Coagulation increased the flux of the UF membrane when removing NOM and particles, and ameliorated the membrane flux recovery after backwashing. The dosage of PAC slightly decreased membrane fouling by particles but effectively increase the submerged membrane flux when removing NOM.

(4) There was an additive effect of membrane fouling by NOM and inorganic particles for the solo UF process. Coagulation in the ultrafiltration hybrid treatment process reduced this additive effect effectively. Particles had a positive effect on relieving membrane fouling in coagulation/UF process.

Acknowledgments

This work was supported by the National Key Technology R&D Program in the 11th-Five Year Plan of China (No. 2006BAD01B03).

References

- Campinas M, Rosa M J, 2010. Assessing PAC contribution to the NOM fouling control in PAC/UF systems. *Water Research*, 44(5): 1636–1644.
- Cho J, Amy G, Pellegrino J, 1999. Membrane filtration of natural organic matter: Initial comparison of rejection and flux decline characteristics with ultrafiltration and nanofiltration membranes. *Water Research*, 33(11): 2517–2526.
- Costa A R, De Pinho M N, 2004. Coagulation/flocculation/ultrafiltration for natural organic matter removal in drinking water production. *Water Science and Technology: Water Supply*, 4(5-6): 215–222.
- Costa A R, De Pinho M N, Elimelech M, 2006. Mechanisms of colloidal natural organic matter fouling in ultrafiltration. *Journal of Membrane Science*, 281(1-2): 716–725.

- Dong B Z, Chen Y, Gao N Y, Fan J C, 2007. Effect of coagulation pretreatment on the fouling of ultrafiltration membrane. *Journal of Environmental Sciences*, 19(3): 278–283.
- Duclos-Orsello C, Li W Y, Ho C C, 2006. A three mechanism model to describe fouling of microfiltration membranes. *Journal of Membrane Science*, 280(1-2): 856–866.
- Howe K J, Marwah A, Chiu K P, Adham S S, 2006. Effect of coagulation on the size of MF and UF membrane foulants. *Environmental Science and Technology*, 40(24): 7908–7913.
- Hu J Y, Shang R, Deng H P, 2010. Evaluation of PAC effect in integrated PAC/UF system for surface water treatment. In: 4th International Conference on Bioinformatics and Biomedical Engineering, iCBBE. Chengdu, China. 18–20 June. 1–4.
- Jermann D, Pronk W, Kägi R, Halbeisen M, Boller M, 2008. Influence of interactions between NOM and particles on UF fouling mechanisms. *Water Research*, 42(14): 3870–3878.
- Kim H C, Hong J H, Lee S, 2006. The fouling of ultrafiltration membranes by natural organic matter after chemical coagulation treatment with different initial mixing conditions. *Water Science and Technology: Water Supply*, 6(4): 117–124.
- Matsui Y, Fukuda Y, Inoue T, Matsushita T, Aoki N, Mima S, 2004. Enhancing an adsorption-membrane hybrid system with microground activated carbon. *Water Science and Technology: Water Supply*, 4(5-6): 189–197.
- Nghiem L D, Oschmann N, Schäfer A I, 2006. Fouling in greywater recycling by direct ultrafiltration. *Desalination*, 187(1-3): 283–290.
- Tomaszewska M, Mozia S, 2002. Removal of organic matter from water by PAC/UF system. *Water Research*, 36(16): 4137–4143.
- Tombácz E, Libor Z, Illés E, Majzik A, Klumpp E, 2004. The role of reactive surface sites and complexation by humic acids in the interaction of clay mineral and iron oxide particles. *Organic Geochemistry*, 35(3): 257–267.
- Xia S J, Liu Y N, Li X, Yao J J, 2007. Drinking water production by ultrafiltration of Songhuajiang River with PAC adsorption. *Journal of Environmental Sciences*, 19(5): 536–539.
- Zhang M M, Li C, Benjamin M M, Chang Y J, 2003. Fouling and natural organic matter removal in adsorbent/membrane systems for drinking water treatment. *Environmental Science and Technology*, 37(8): 1663–1669.
- Zhao P, Takizawa S, Katayama H, Ohgaki S, 2005. Factors causing PAC cake fouling in PAC-MF (powdered activated carbon-microfiltration) water treatment systems. *Water Science and Technology*, 51(6-7): 231–240.